

Short Communication

Corrosion Resistance of Niobium Microalloyed HRB500 Mild Steel Rebar in the Alkaline Concrete Pore Solution

Hongzhi Liu¹, Longjiang Wang^{2,*}, Jiakai Sun³, Weijian Liu⁴, Zhenwei Wang⁵

¹ Shandong Urban Construction Vocational College, Jinan, 250103, China

² College of River and Ocean Engineering, Chongqing Jiaotong University, Chongqing, 400074, China

³ China Coal Research Institute, Beijing 100013, China

⁴ Department of Architecture and Engineering, Zhongyuan University of Technology, Zhengzhou 450007, China

⁵ School of Civil Engineering, North China University of Technology, Beijing, 100144, China,

*E-mail: bylongjiang@126.com

Received: 4 february 2020 / Accepted: 27 March 2020 / Published: 10 June 2020

Recently, micro-alloyed steel rebars had been evaluated extremely to improve corrosion resistance of steel rebars in corrosive environments which intended to enhance the service life of reinforced concrete structures. In this study, corrosion resistance of niobium (Nb) microalloyed HRB500 mild steel rebar in the alkaline concrete pore solution were investigated by electrochemical technique. Electrochemical impedance spectroscopy (EIS), cyclic voltammetry (CV) and potentiodynamic polarization techniques were used to study the effect of Nb content on corrosion behavior of steel rebars. The CV results showed that the current density in zero potential decreased by increasing the Nb content, indicating that a small amount of Nb microalloy in steel rebars facilitated the stability of the formed passive layers. The polarization plots showed that the steel rebar with 0.055 wt% Nb content had a smaller corrosion current-density than the other samples which was in the passive state during the test. The EIS results indicated that the double-layer capacitance value decreased with the addition of Nb content, resulting in enhanced protective capacity. The surface morphology of the samples revealed that the surface of steel rebar with 0.055 wt% Nb was smooth and no visible corrosion was observed.

Keywords: Corrosion resistance; Niobium microalloyed steel rebar; Electrochemical impedance spectroscopy; Simulated concrete pore solution

1. INTRODUCTION

Corrosion of steel bars is one of the problems that need further evaluation to improve the corrosion condition. Because concrete has a high alkaline environment, steel bars are not exposed to

corrosion for a short period of time [1, 2]. The passive layer on the surface of carbon steel rebars is stable in the alkaline environment [3]. However, the chloride ions in the concrete after a long period of time results in the weakening of the modified concrete structures [4, 5]. It seems that the existence of carbonation causes a uniform passivation of steel rebars because of the $\text{CO}_3^{2-}/\text{HCO}_3^-$ at a the specific pH value [6]. Several environmental factors such as NO_2 and SO_2 in acid rain and CO_2 in the air pollutions lead to the reduction of concrete alkalinity [7]. These environmental factors could react with calcium hydroxide and calcium-silicate-hydrate gel in the concrete [8, 9]. Today, low-alloy steel rebars are alternative techniques to promote corrosion resistance. Niobium (Nb) is one of the elements employed in low-alloy steel rebars. Xu et al. [10] showed that the Ti_5Si_3 corrosion resistance was promoted with the increase of Nb content in H_2SO_4 solution. Sun et al. [11] suggest that the addition of Nb in steel rebars can lead to a satisfactory performance to enhance the corrosion resistance of stainless steel. OrjuelaG et al. [12] improved corrosion resistance of rebars by coating niobium carbide on the surface of a low-alloy steel. Many strategies have been adopted to improve the corrosion behavior of steel rebars in corrosive environments. However, studies on niobium content in a steel rebar in an alkaline concrete pore solution by the electrochemical process have not yet been published. Thus, in this study, the effect of niobium content on steel rebar corrosion in alkaline concrete pore solution were investigated. The cyclic voltammetry, electrochemical impedance spectroscopy and potentiodynamic polarization techniques were utilized to study the electrochemical properties of Nb microalloyed HRB500 mild steel rebar in alkaline concrete pore solution.

2. MATERIALS AND METHOD

In this work, HRB500 mild steel with 25 mm diameter were used to study the corrosion behavior of niobium (Nb) microalloyed steel rebar in alkaline environment. Table 1 indicates the chemical composition of the mild steel rebars used in this work.

Table 1. Chemical composition of mild steel rebars with different Nb content (wt%)

Steels	C	Mn	Si	P	S	Nb	Fe
Sample A	0.32	1.63	0.51	0.02	0.024	0.0	Residual
Sample B	0.32	1.63	0.52	0.02	0.024	0.025	Residual
Sample C	0.32	1.63	0.53	0.02	0.024	0.04	Residual
Sample D	0.32	1.63	0.52	0.02	0.024	0.055	Residual

The Nb contents were varied from 0.0 wt% to 0.055 wt%. The samples were cleaned and polished by using SiC grinding papers. All samples were cleaned in acetone in an ultrasonic cleaner (Mophorn, China) and washed in distilled water.

The alkaline concrete pore solution was prepared using 0.75 g L^{-1} $\text{Ca}(\text{OH})_2$, 0.75 g L^{-1} NaOH , and 5 g L^{-1} of KOH . The weight fraction of sodium chloride in the solution was 1.5 wt%. The pH was adjusted to 13.0 with the addition of NaHCO_3 solutions and calibrated by a pH meter.

The homemade electrochemical cell was used to study on the electrochemical impedance spectroscopy (EIS) of the samples. In the three-electrode system, steel rebar samples were used as a working electrode and a saturated calomel electrode was applied as a reference electrode. The graphite was used as the counter electrode. Before analysing the samples, all samples were immersed in a prepared solution for 25 minutes. A copper wire was connected to the ends of the steel rebar samples. EIS characterizations were performed in the varied frequency between 100 kHz and 0.1 mHz at the E_{OC} with AC perturbation ± 10 mV. The potentiodynamic polarization (CorrTest Instruments Corp., Ltd., China) measurement was conducted from 0.25V at 1 mV/s scanning rate. The cyclic voltammetry analysis was carried out between -1.5V and 1.5 V at scan rate with 50 mV/s and recorded sixth cyclic voltammograms for making comparison between the samples.

3. RESULTS AND DISCUSSION

In order to study the redox reactions and formation of the passive layer on the sample in the alkaline environment, cyclic voltammetry (CV) technique was used. Figure 1 shows the cyclic voltammograms of the samples in the simulated concrete pore solution with pH value of 12. The anodic and cathodic peak potentials were observed as shown in Figure 1.

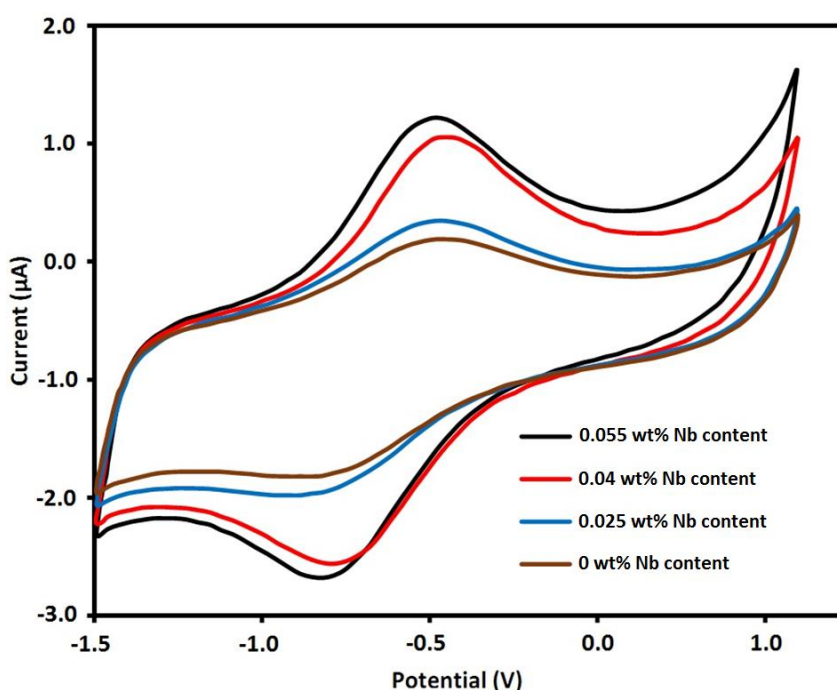
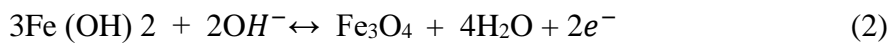


Figure 1. Cyclic voltammograms of the samples with different Nb content exposed to the simulated concrete pore solution with pH value of 13.

The anodic peak appeared at an approximate potential of -0.65 V for all samples that is related to the following reactions from (1) to (3). It confirms the transformation from Fe^{2+} to Fe^{3+} ions and the passive layer formation on the surface of steel rebars [13]:



As previously reported, the current density in zero potential (i_0) can exhibit the corrosion behavior of passive layer [14]: the higher i_0 proposes poorer corrosion resistance. When Nb content increases, i_0 decreases. This reduction indicates that a small amount of Nb micro-alloy in steel rebars facilitates the stability of the formed passive layers. As the potential increases up to 0.3 V, the anodic current-density suddenly increases which can be related to the electrochemical process controlled by oxygen evolution. As shown in figure 1, the cathodic peak appears at the potential of -0.85 V. When the potential shifts to a more negative value, the cathodic current density increases rapidly which can be associated to the electrochemical process controlled by hydrogen evolution [15]. Furthermore, the anodic peak of 0.055 wt% Nb steel rebar is lower than the other samples. It can be concluded that the increase in Nb content in steel rebar can enhance corrosion resistance and stability of passive film.

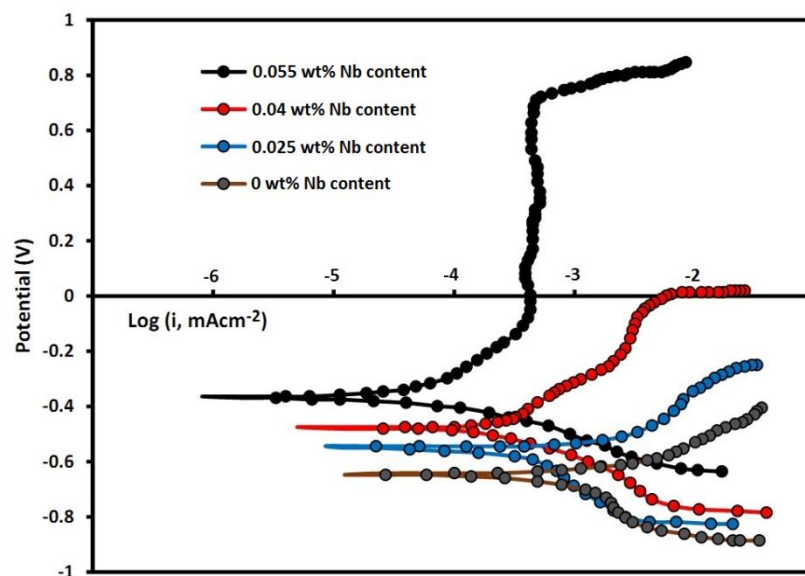


Figure 2. Potentiodynamic polarization plots of the samples with different Nb content exposed to the simulated concrete pore solution with pH value of 13.

Potentiodynamic polarization is a technique where the potential of the electrode is varied at a selected rate by application of a current through the electrolyte. From polarization plots in Figure 2, sample D (0.055 wt% Nb content) shows noticeable passivation in the solution and the most positive in pitting potential.

The Butler-Volmer equation can describe the polarization potential (E)-current density (I) relation in potentiodynamic polarization condition [16]:

$$I = I_{corr} \left\{ \exp \left[\frac{\alpha_a z F}{RT} (E - E_{corr}) \right] - \exp \left[-\frac{\alpha_c z F}{RT} (E - E_{corr}) \right] \right\} \quad (4)$$

Where I_{corr} and E_{corr} are the current density and potential of corrosion, respectively. α_c and α_a are cathodic and anodic charge transfer coefficient, respectively, which indicate corrosion mechanism and kinetics. z refers to the electron number that participated in reactions, F is Faraday constant (96485.33212 C mol⁻¹) and R is universal gas constant (8.31446261815324 J K⁻¹ mol⁻¹). These parameters can be estimated by a curve-fitting method in the weak-polarization behavior for the samples [17]. Furthermore, anodic and cathodic sites on rebar surfaces lead to the development of a potential difference, which is the driving force behind corrosion reactions that are electrochemical in nature. Non-homogeneous chemistry, variations of grain size, the presence of non-uniform residual stresses generated in rebar during manufacturing processes cause anodic and cathodic sites on rebar surfaces. Table 2 presents the corrosion potential and corrosion current density of the samples.

Table 2. Fitting parameters of the samples obtained from polarization plots.

Steel	Corrosion current density (μAcm^{-2})	Corrosion potential (V)
Sample A	0.184	-0.643
Sample B	0.165	-0.534
Sample C	0.145	-0.472
Sample D	0.096	-0.365

As shown in table 3, the corrosion level can be defined into four levels proposed by Durar Network Specification [18].

Table 3. Corrosion level

Corrosion level	Corrosion current density (i_{corr}) range
Very high	$1.0 \mu\text{A/cm}^2 < i_{corr}$
High	$0.5 \mu\text{A/cm}^2 < i_{corr} < 1.0 \mu\text{A/cm}^2$
Low	$0.1 \mu\text{A/cm}^2 < i_{corr} < 0.5 \mu\text{A/cm}^2$
Passivity	$i_{corr} < 0.1 \mu\text{A/cm}^2$

However, based on table 3, the corrosion current density of sample D in concrete pore solution is lower than that of the other samples. Therefore, mild steel rebar steel (sample D) remained completely in the passive state during the test which indicated their good corrosion resistance in the alkaline concrete pore solution [19, 20].

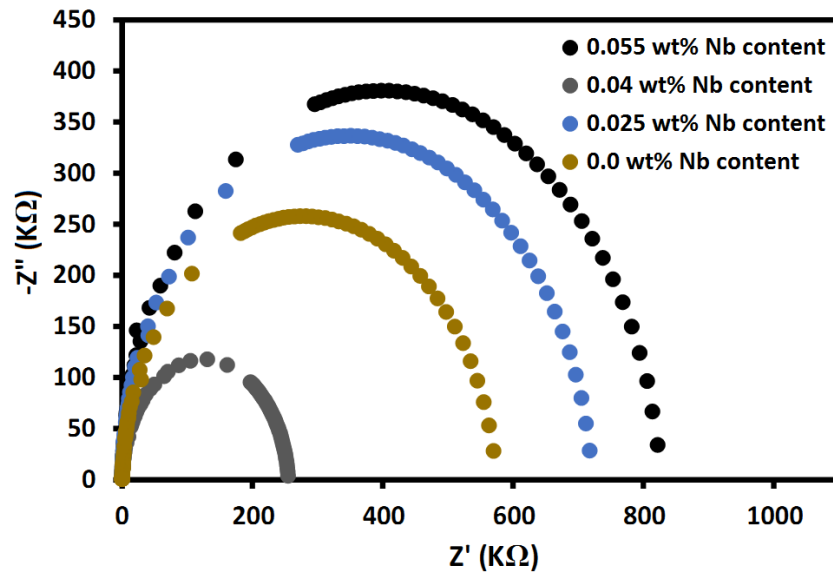


Figure 3. EIS curves of the rebars with different concentrations of Nb exposed to the simulated concrete pore solution with 13 pH value.

For further study of the effect of Nb micro-alloy amount on the corrosion behavior of rebars with passive layers in simulated concrete pore solution, EIS was measured and shown in Figure 3. The increase in Nb content leads to an increase in the radius of the capacitive loop which indicates enhancement of the corrosion resistance for steel rebar. Figure 4 indicates an equivalent circuit used to model the impedance spectra. R_s is the solution resistance. R_f and R_{ct} are the resistance of passive film and the charge-transfer resistance, respectively [21]. CPE_f and CPE_{dl} are the passive film/solution interface capacitance and double-layer capacitance [22].

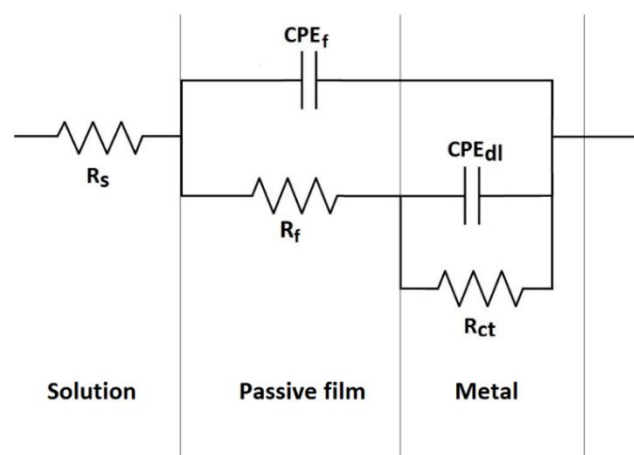


Figure 4. An equivalent circuit model to fit the experimental data

Polarization resistance, R_p ($R_p = R_f + R_{ct}$) is a measurable indicator to characterize the corrosion resistance of steel in corrosive environment, and the higher R_p corresponds to the better corrosion resistance.

Table 4. Electrochemical parameters from the fitting using the equivalent circuit in Figure 4 for pH value of 13 and various content of Nb

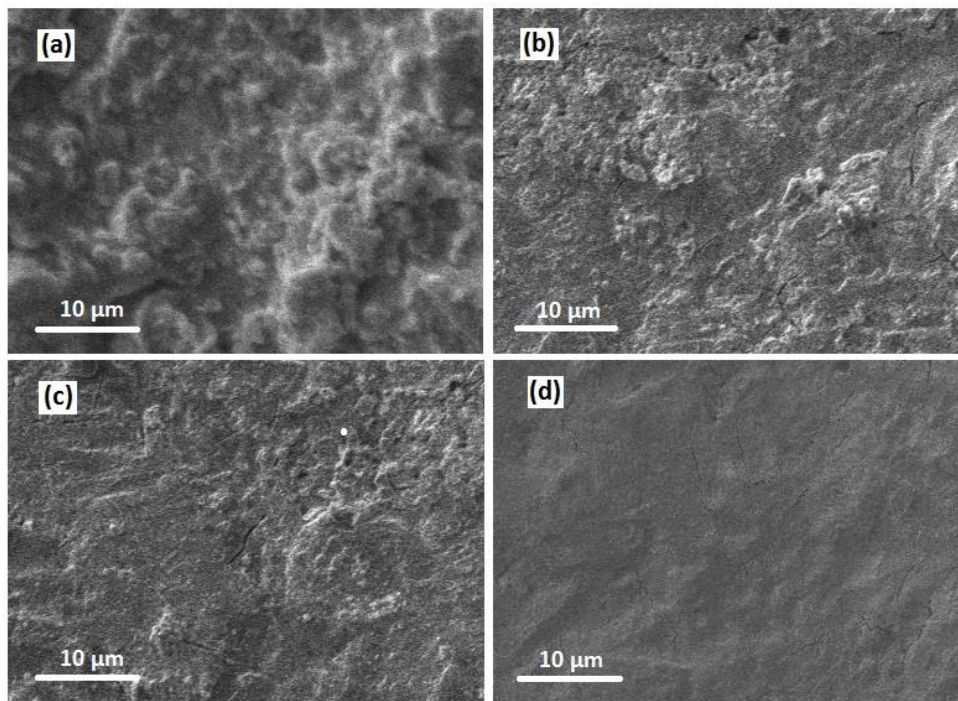
Steels	R_s (Ω cm ²)	R_f ($M\Omega$ cm ²)	CPE_f (μF cm ⁻²)	R_{ct} ($M\Omega$ cm ²)	CPE_{dl} (μF cm ⁻²)
Sample A	27.4	0.178	2.6	0.252	3.2
Sample B	23.2	0.346	2.3	0.582	2.8
Sample C	41.3	0.412	1.7	0.732	2.1
Sample D	34.5	0.583	1.2	0.826	1.8

According to table 4, increasing the Nb contents show a significantly enhancement in R_p value indicating a higher corrosion resistance for 0.055 wt% Nb steel rebar in pH 13.

CPE_f is related to the thickness of passive film as shown in the following formula [23]:

$$CPE_f = \frac{\varepsilon\varepsilon_0A}{D_p} \quad (5)$$

where ε_0 is used to represent the permittivity of vacuum, A for effective area, ε for dielectric constant, and D_p for the thickness of passive film which can be qualitatively described with CPE_f .

**Figure 5.** FESEM images of the samples with different content of Nb, (a) 0 wt%, sample A (b) 0.025 wt%, sample B (c) 0.04 wt%, sample C and (d) 0.055 wt%, sample D.

The value of CPE_f decreases as the Nb content increases (table 4), which indicates that the passive film thickness increased and the resulting protective capacity enhanced when the Nb content of steel rebar gradual increased. In pH value of 13, the R_f passive film resistance increased as the Nb

content in alloy increased, which indicates that the protective feature of the passive film developed is strong. Compared to CPE_f and CPE_{dl} , it was found that CPE_f is lower than CPE_{dl} which confirm that the formation of thin passive film and the double layer at the interfaces has a high capacitive behavior.

Figure 5 reveals the FESEM morphology of rebars after the immersion in the simulated concrete pore solution at pH of 13 for 30 days. Wide corrosion occurred on the surface of sample A and B, indicating the active corrosion state. Moreover, a number of small pits can be observed on the surface of sample C. The surface of sample D was clean and smooth without any visible corrosion areas, indicating that the samples C and D had a suitable corrosion resistance even in the simulated concrete pore solution. These findings reveal that the addition of Nb enhances the corrosion resistance which is in agreement with the results of electrochemical measurements.

4. CONCLUSIONS

Recent studies showed that the micro-alloyed steel rebars can improve the corrosion behavior of steel reinforced concretes in an aggressive environment. Here, Nb as an alloying element was selected to investigate the alloy effects on corrosion resistance of mild steel rebar in the alkaline concrete pore solution. FESEM images indicated that the surface of steel rebar with 0.055 wt% Nb was smooth and no visible corrosion was observed. The CV results showed that the current density in zero potential decreased by increasing the Nb content, indicating a small amount of Nb microalloy in steel rebars facilitated the stability of the formed passive layers. The polarization plots showed that the steel rebar with 0.055 wt% Nb content had a smaller corrosion current-density than the other samples which was in the passive state during the test. The EIS results indicated that double-layer capacitance value decreased with the addition of Nb content, resulting in an enhanced protective capacity.

ACKNOWLEDGEMENT

This work was sponsored in part by the Natural Science Foundation of Henan Province(182300410161), the National Natural Science Foundation of China (51774184), the Excellent Research Team Fund in North China University of Technology (Grant No. 107051360019XN134/017), and the Scientific Research Fund in North China University of Technology (Grant No. 110051360002).

References

1. D. Shen, *International Journal of Electrochemical Science*, 14 (2019) 6513.
2. V. Marcos-Meson, A. Michel, A. Solgaard, G. Fischer, C. Edvardsen and T.L. Skovhus, *Cement and Concrete Research*, 103 (2018) 1.
3. M. Mancio, G. Kusinski, P. Monteiro and T. Devine, *Journal of ASTM International*, 6 (2009)
4. R.D. Moser, P.M. Singh, L.F. Kahn and K.E. Kurtis, *Corrosion Science*, 57 (2012) 241.
5. F. Husairi, J. Rouhi, K. Eswar, A. Zainurul, M. Rusop and S. Abdullah, *Applied Physics A*, 116 (2014) 2119.
6. M.B. Valcarce and M. Vázquez, *Materials Chemistry and Physics*, 115 (2009) 313.

7. M. Pandiarajan, P. Prabhakar and S. Rajendran, *European Chemical Bulletin*, 1 (2012) 238.
8. Q. Chen, Y. Ke, L. Zhang, M. Tyrer, C.D. Hills and G. Xue, *Journal of hazardous materials*, 166 (2009) 421.
9. R. Dalvand, S. Mahmud and J. Rouhi, *Materials Letters*, 160 (2015) 444.
10. J. Xu, L. Liu, I. Zhengyang, P. Munroe and Z.H. Xie, *Acta Materialia*, 63 (2014) 245.
11. T. Sun, B. Deng, J. Xu, J. Li and Y. Jiang, *Journal of Chinese Society for Corrosion and Protection*, 30 (2010) 421.
12. A. OrjuelaG, R. Rincón and J.J. Olaya, *Surface and Coatings Technology*, 259 (2014) 667.
13. E. Volpi, A. Olietti, M. Stefanoni and S.P. Trasatti, *Journal of Electroanalytical Chemistry*, 736 (2015) 38.
14. C. Wang, S. Yang, Y. Chen, B. Wang, J. He and C. Tang, *RSC Advances*, 5 (2015) 34580.
15. M. Alimanesh, J. Rouhi and Z. Hassan, *Ceramics International*, 42 (2016) 5136.
16. R. Wang, S. Luo, M. Liu and Y. Xue, *Corrosion Science*, 85 (2014) 270.
17. J.W. Wu, D. Bai, A. Baker, Z.H. Li and X.B. Liu, *Materials and corrosion*, 66 (2015) 143.
18. W. Zhao, J. Zhao, S. Zhang and J. Yang, *International Journal of Electrochemical Science* 14 (2019) 8039.
19. A.T. Yousefi, S. Ikeda, M.R. Mahmood, J. Rouhi and H.T. Yousefi, *World Applied Sciences Journal*, 17 (2012) 524.
20. J. Rouhi, M.R. Mahmood, S. Mahmud and R. Dalvand, *Journal of Solid State Electrochemistry*, 18 (2014) 1695.
21. F. Husairi, J. Rouhi, K. Eswar, C.R. Ooi, M. Rusop and S. Abdullah, *Sensors and Actuators A: Physical*, 236 (2015) 11.
22. H. Luo, C. Dong, X. Li and K. Xiao, *Electrochimica Acta*, 64 (2012) 211.
23. V. Maurice, H. Peng, L.H. Klein, A. Seyeux, S. Zanna and P. Marcus, *Faraday discussions*, 180 (2015) 151.